# Probing a black-bounce, traversable wormhole with weak deflection gravitational lensing

Xiao-Tong Cheng and Yi Xie*

*School of Astronomy and Space Science, Nanjing University, Nanjing 210023, China and Key Laboratory of Modern Astronomy and Astrophysics, Nanjing University, Ministry of Education, Nanjing 210023, China*

(Received 28 September 2020; accepted 25 February 2021; published 22 March 2021)

In the strong deflection gravitational lensing, given the fact that a black-bounce, traversable wormhole is indistinguishable from a Schwarzschild black hole and is loosely tested by the Event Horizon Telescope, we intensively study its signatures of weak deflection gravitational lensing in light of the tremendous progress made by the new generation of the near-infrared interferometer GRAVITY. After obtaining its observables, which are the positions, magnitudes of brightness, centroid, and differential time delay between the lensed images, we investigate three astrophysical scenarios: an orbiting star lensed by the Galactic Center Sgr A*, a microlensed star in the Galactic bulge, and microlensing by a nearby lens. We find that the measurements of the observables of Sgr A* provide a promising way to test the black-bounce, traversable wormhole spacetime. GRAVITY can resolve the angular separation, the angular difference, and the time delay between the two lensed images by Sgr A*, and it can marginally detect their deviations from those of the Schwarzschild black hole. The brightness difference between the images and its deviation might be measured by a dedicated space telescope. In the near future, we expect that such a spacetime would be more robustly tested with the weak deflection gravitational lensing by further improved and upgraded GRAVITY+.

DOI: 10.1103/PhysRevD.103.064040

## I. INTRODUCTION

Black holes are found to be common in the Universe by detecting gravitational waves from them [1–6] and by imaging the center of galaxy M87 [7–12]. They also provide ideal laboratories for testing fundamental theories of gravity in the strong field. Predicted by Einstein's general relativity, a black hole is the simplest celestial body, whereas the event horizon and central singularity also poison it, respectively, by causing the information-loss problem and by making general relativity invalid. In order to remove the singularity, lots of proposals have been made, including constructing a regular core [13–16], bouncing via the quantum pressure [17–19], and making a quasiblack hole [20–23] (see Ref. [24] for a review).

Recently, a black-bounce, traversable wormhole spacetime was introduced [25], and it interpolates between a regular black hole (a black bounce) and a traversable wormhole controlled by a parameter of length $a_\bullet$. When its mass vanishes, it returns to the Ellis wormhole [26]. Such a spacetime has drawn much attention due to its interesting characteristics. It was extended to a time-dependent spacetime [27], and a spherically symmetric thin-shell traversable wormhole was constructed based on it [28]. Its quasinormal modes [29] and its absorption of massless scalar waves [30] were studied.

With a deflection angle much bigger than 1, the strong deflection gravitational lensing by the black-bounce, traversable wormhole was intensively investigated [31,32]. It was found [31] that the shadow cast by the black-bounce, traversable wormhole with mass $m_\bullet$ and $a_\bullet \in (0, 3m_\bullet)$ ($G = c = 1$) has exactly the same apparent size as the one of the Schwarzschild black hole with the same mass and distance, while the separations of its relativistic images from the photon sphere are too small to determine with current angular resolution, not to mention their even much smaller deviations from those of the Schwarzschild black hole and their exceeding faintness. Therefore, the black-bounce, traversable wormhole is indistinguishable from the Schwarzschild black hole in the strong deflection gravitational lensing for such a parameter range of $a_\bullet$. After confirming these statements, the work of Ref. [32] made an extension by studying its strong deflection gravitational lensing for the cases of $a_\bullet \geq 3m_\bullet$ and obtained a bound as $a_\bullet = (4.2 \pm 0.6)m_\bullet$ based on the angular diameter of M87*'s shadow observed by the Event Horizon Telescope (EHT) [7]. Such a strong-field test does not reject the possibility that M87* is a wormhole [32].

Although the observed shadow of M87* by EHT was employed for various gravitational tests of the black-hole

* yixie@nju.edu.cn

 

metric in the strong-field regime [33], it was recently pointed out [34] that the appearance of M87* currently measured by the Earth-sized EHT cannot be used to test general relativity. The interpretation of such an observation depends heavily on general relativistic magnetohydrodynamic simulations using the Kerr spacetime with many untested assumptions about accretion flow and emission physics, so that any difference from the Kerr spacetime, such as the deviation in the spacetime caused by the black-bounce, traversable wormhole cannot be told from the violation of the relevant astrophysical assumptions. The photon ring [35] originated by photons orbiting M87* can provide a robust test bed, whereas it has to wait for very challenging space-based interferometry available [36–38]. Therefore, given the aforementioned facts, they suggest that the black-bounce, traversable wormhole would unlikely be tested through the strong deflection gravitational lensing in the near future.

Even though it seems to be contrary to expectation at first glance, the weak deflection gravitational lensing might be a promising way to test the black-bounce, traversable wormhole spacetime due to tremendous advances achieved by and prospects of the new generation of a near-infrared interferometer. With a deflection angle much less than 1, the weak deflection gravitational lensing has long since been an important tool in astronomy [39–42] and gravitational physics [43–48]. The gravitational lensing by the Ellis wormhole [49–56], by various kinds of wormholes [57–59], and by black holes [60–70] has been widely studied. In practice, the feasibility of testing the black-bounce, traversable wormhole spacetime with the weak deflection gravitational lensing is raised and driven by the instrument GRAVITY, which can coherently combine the light of the European Southern Observatory Very Large Telescope Interferometer and work as a telescope with an equivalent 130 m diameter angular resolution [71]. In a largely self-contained way, GRAVITY can be used for phase-referenced imaging of faint targets and precise narrow angle astrometry. Since 2017, it has been routinely monitoring the Galactic Center, especially following the supermassive black-hole candidate Sgr A* and the star S2 [71,72]. It has detected the gravitational redshift [73] and the Schwarzschild precession [74] in the orbit of S2 around Sgr A*. Among these detections, its extremely accurate astrometry down to ~10 microarcsecond ($\mu$as), depending on the brightness of the targets and the integration time (typically 10 s for an individual exposure), plays a critical role [71,72]. As we will show, GRAVITY already has the ability to marginally detect the deviations of the observables in the weak deflection gravitational lensing caused by the black-bounce, traversable wormhole from those of the Schwarzschild black hole for Sgr A*. With further improvement [75], future upgrades of the GRAVITY + project and detection of faint stars in a projection passing closer to Sgr A* than S2 [76], it can be expected that this instrument provides a very hopeful way to test the black-bounce, traversable wormhole in the near future.

Nevertheless, the signatures of the weak deflection gravitational lensing by the black-bounce, traversable wormhole are still unknown, except that the bending angle up to the leading order was given by Refs. [31,32], presenting very limited information. In order to find these missing puzzle pieces, which might provide crucial clues for searching and detecting such a spacetime, we intensively examine the weak deflection gravitational lensing by the black-bounce, traversable wormhole with the well-established method introduced by Keeton and Petters [43–45] and detailedly analyze its observability for several astrophysical scenarios.

In Sec. II, we briefly review the spacetime of the black-bounce, traversable wormhole and work out its bending angle up to the third order to lay the foundation for the following works. In Sec. III, we investigate its weak deflection gravitational lensing and obtain its practical observables. We discuss its observability for three astrophysical cases in Sec. IV. Finally, in Sec. V, we conclude and discuss our results.

## II. SPACETIME AND LIGHT DEFLECTION

### A. Spacetime

The spacetime of a static black-bounce, traversable wormhole spacetime with mass $m_\bullet$ reads ($G = c = 1$) [25]

$$ds^2 = -A(r)dt^2 + B(r)dr^2 + C(r)(d\theta^2 + \sin^2\theta d\phi^2), \quad (1)$$

where

$$A(r) = [B(r)]^{-1} = 1 - \frac{2m_\bullet}{\sqrt{r^2 + \alpha_\bullet^2}}, \quad (2)$$

$$C(r) = r^2 + \alpha_\bullet^2, \quad (3)$$

and $\alpha_\bullet$ is a parameter with the dimension of length. When $\alpha_\bullet = 0$, it is the Schwarzschild black hole, when $0 < \alpha_\bullet < 2m_\bullet$ it is a black bounce with a one-way spacelike throat, and with an event horizon at [25]

$$r_H = \sqrt{4m_\bullet^2 - \alpha_\bullet^2} \quad (4)$$

when $\alpha_\bullet = 2m_\bullet$, it is a one-way wormhole with a null throat, and when $\alpha_\bullet > 2m_\bullet$, it is a traversable wormhole in the Morris-Thorne sense. When $\alpha \neq 0$, the spacetime (1) is regular at $r = 0$, and it is asymptotically flat as $r \to +\infty$. When the mass of the black-bounce, traversable wormhole vanishes, the spacetime (1) returns to the Ellis wormhole [26] whose gravitational lensing signals have been widely examined in the weak [49–56] and strong [77–79] deflection cases and whose observational bound has been well established [80]. When $\alpha \in (2, 3)$, the black-bounce,

traversable wormhole will be a candidate for ultracompact object s with the photon spheres [81], which are more massive than neutron stars but without the event horizon. The gravitational lensing of other kinds of the ultracompact object s has been widely studied [82–98].

This black-bounce, traversable wormhole spacetime can cast a shadow in direct imaging observations with the angular radius as [31,32]

$$\theta_\infty = \frac{m_\bullet}{D_{\rm OL}} \times \begin{cases} 3\sqrt{3}, & 0 < \alpha \leq 3, \\ \sqrt{\frac{\alpha^3}{\alpha-2}}, & \alpha > 3, \end{cases} \tag{5}$$

where $D_{\rm OL}$ is its distance to the observer, and we define a dimensionless parameter as

$$\alpha = \frac{\alpha_\bullet}{m_\bullet}. \tag{6}$$

For $\alpha \in (0, 3]$, the apparent size of the shadow is identical to the one of the Schwarzschild black hole with the same $m_\bullet$ and $D_{\rm OL}$. It can also generate relativistic images, which separate from the silhouette of the shadow less than 0.3 $\mu$as by taking the supermassive black hole at the Galactic Center, Sgr A*, as the lens [31]. However, these small separations of the relativistic images are far beyond the current angular resolutions of astronomical observations. These facts make the black-bounce, traversable wormhole indistinguishable from the Schwarzschild black hole in the strong deflection gravitational lensing for this range of $\alpha$. In the domain $\alpha > 3$, according to the observed angular diameter of M87*'s shadow by EHT [7], a preliminary bound on $\alpha$ was obtained as [32]

$$\alpha = 4.2 \pm 0.6, \tag{7}$$

which does not reject the wormhole cases. Nevertheless, as pointed in Ref. [34], this bound cannot be treated as a genuine constraint on the black-bounce, traversable wormhole spacetime since the observation by EHT depends on plenty of assumptions, making it hard to tell whether the spacetime predicted by general relativity or the astrophysical assumptions on accretion flow and emission physics were broken in this test. A more robust test in this trial would have to wait for the flight of a very challenging space-borne interferometer [38]. Therefore, inspired by the progress of the near-infrared interferometer GRAVITY [71], we dedicate ourselves to an intensive study of the weak deflection gravitational lensing by the black-bounce, traversable wormhole to search and detect them.

For later convenience, we define a dimensionless parameter

$$q = \alpha^2. \tag{8}$$

In order to ensure that the parameter space of $q$ includes the subdomain with the observables of the strong deflection gravitational lensing indistinguishable from those of the Schwarzschild black hole and the bound on $\alpha$ given by EHT, we will consider a bigger domain as

$$\mathcal{D} = \{q | 0 < q \leq 25\} \tag{9}$$

and pay particular attention to its EHT-allowed subdomain for the wormhole deduced by Eq. (7),

$$\mathcal{D}_{\rm EHT} = \{q | 12.6 \leq q \leq 22.7\}. \tag{10}$$

We expect that for $q \in (0, 9]$, which makes the black-bounce, traversable wormhole have the same shadow as the Schwarzschild black hole, its observables in the weak deflection gravitational lensing would still be very challenging to detect; however, for $q \in \mathcal{D}_{\rm EHT}$, its observables might be marginally detected by GRAVITY and would be more reliably measured by the next generation of GRAVITY+.

### B. Light deflection

For the black-bounce, traversable wormhole spacetime (1), the exact bending angle of a deflected light ray can be obtained as [99,100]

$$\hat{\alpha}(r_0) = 2\int_{r_0}^{\infty} \frac{\sqrt{B(r)}}{\sqrt{C(r)}\sqrt{\frac{C(r)}{C(r_0)}\frac{A(r_0)}{A(r)} - 1}} {\rm d}r - \pi, \tag{11}$$

where $r_0$ is the closet approach distance of the photon. In the case of weak deflection gravitational lensing, since $r_0$ is much larger than $\sim m_\bullet$, the bending angle will be significantly smaller than 1 so that we can find the deflection angle in terms of $m_\bullet r_0^{-1}$ as

$$\hat{\alpha}(r_0) = 4\frac{m_\bullet}{r_0} + \left(\frac{15}{4}\pi - 4 + \frac{\pi}{4}q\right)\left(\frac{m_\bullet}{r_0}\right)^2 + \left[\frac{122}{3} - \frac{15}{2}\pi + \left(\frac{2}{3} - \frac{\pi}{2}\right)q\right]\left(\frac{m_\bullet}{r_0}\right)^3 + \mathcal{O}\left(\frac{m_\bullet^4}{r_0^4}\right). \tag{12}$$

When $q$ vanishes, this deflection angle returns to the one caused by the Schwarzschild black hole [43]. It is well known that $r_0$ depends on the choice of coordinates while the impact parameter $u$ is gauge invariant and satisfies that

$$u^2 = \frac{C(r_0)}{A(r_0)}. \tag{13}$$

Therefore, we can find $r_0$ as

$$\frac{r_0}{u} = 1 - \frac{m_\bullet}{u} - \left(\frac{3}{2} + \frac{q}{2}\right)\left(\frac{m_\bullet}{u}\right)^2 - \left(4 + \frac{q}{2}\right)\left(\frac{m_\bullet}{u}\right)^3 + \mathcal{O}\left(\frac{m_\bullet^4}{u^4}\right), \tag{14}$$

and replace it with $u$ in the deflection angle, which leads to

$$\hat{\alpha}(u) = 4\frac{m_\bullet}{u} + \left(\frac{15}{4} + \frac{q}{4}\right)\pi\left(\frac{m_\bullet}{u}\right)^2 + \left(\frac{128}{3} + \frac{8}{3}q\right)\left(\frac{m_\bullet}{u}\right)^3 + \mathcal{O}\left(\frac{m_\bullet^4}{u^4}\right). \tag{15}$$

It will be used to obtain observables in the weak deflection gravitational lensing by the black-bounce, traversable wormhole spacetime.

## III. WEAK DEFLECTION GRAVITATIONAL LENSING

In order to find the lensing observables, the lens equation is an indispensable ingredient. We assume that both the source and the observer are in the asymptotically flat regions so that the lens equation is adopted as [99,101]

$$\tan\mathcal{B} = \tan\vartheta - D[\tan\vartheta + \tan(\hat{\alpha} - \vartheta)], \tag{16}$$

where $\mathcal{B}$ and $\vartheta$ are, respectively, the angular positions of the source and the image, $D = D_{\rm LS}/D_{\rm OS}$ with $D_{\rm LS}$ and $D_{\rm OS}$ being the distances from the lens to the source and from the observer to the source projected on the optical axis.

For convenience in the following works, we define the scaled variables [43–45]

$$\beta = \frac{\mathcal{B}}{\vartheta_{\rm E}}, \qquad \theta = \frac{\vartheta}{\vartheta_{\rm E}}, \qquad \varepsilon = \frac{\vartheta_\bullet}{\vartheta_{\rm E}}, \tag{17}$$

where $\vartheta_\bullet = \arctan(m_\bullet/D_{\rm OL})$ is the angular gravitational radius at distance $D_{\rm OL}$, and the angular Einstein ring radius is

$$\vartheta_{\rm E} = \sqrt{\frac{4m_\bullet D_{\rm LS}}{D_{\rm OL}D_{\rm OS}}}. \tag{18}$$

Since both the observer and the source are assumed to be far from the lens, $\varepsilon$ can be treated as a small parameter.

### A. Image positions

Based on the small parameter $\varepsilon$, the position of a lensed image can be written in a series as

$$\theta = \theta_0 + \varepsilon\theta_1 + \varepsilon^2\theta_2 + \mathcal{O}(\varepsilon^3), \tag{19}$$

where $\theta_0$, $\theta_1$, and $\theta_2$ are, respectively, its zeroth-, first-, and second-order approximations. After substituting it into the lens equation (16) and rearranging the resulting lens equation, we find that

$$\theta_0 = \frac{1}{2}(\beta + \eta), \tag{20}$$

$$\theta_1 = \frac{\pi(15+q)}{16(\theta_0^2+1)}, \tag{21}$$

$$\theta_2 = \frac{1}{\theta_0(\theta_0^2+1)^3}\left\{\frac{8}{3}D^2\theta_0^8 + D\left(\frac{64}{3}D - 16\right)\theta_0^6 + \left(\frac{88}{3}D^2 - 32D + 16\right)\theta_0^4 + \left(\frac{16}{3}D^2 - 16D + 32 - \frac{225}{128}\pi^2\right)\theta_0^2 - \frac{16}{3}D^2 + 16 - \frac{225}{256}\pi^2 + \left[\frac{2}{3}\theta_0^4 + \left(\frac{4}{3} - \frac{15}{64}\pi^2\right)\theta_0^2 + \frac{2}{3} - \frac{15}{128}\pi^2\right]q - \frac{\pi^2}{256}q^2(2\theta_0^2+1)\right\}, \tag{22}$$

with

$$\eta = \sqrt{\beta^2 + 4}. \tag{23}$$

The black-bounce, traversable wormhole has the same behavior on the leading order of the image position $\theta_0$ as the Schwarzschild black hole does [43], while these two spacetime s depart from each other from the next-to-leading-order term $\theta_1$ due to the appearance of $q$. When $q = 0$, $\theta_1$ and $\theta_2$ return to those of the Schwarzschild black hole [43].

In this work, we adopt the convention [43] that the angular positions of the lensed images are positive. Thus, if the image is on the same side of the lens as the source, the position of the source is positive; otherwise, it is negative. The positive- and negative-parity images can be found at each order as

$$\theta_0^{\pm} = \frac{1}{2}(\eta \pm |\beta|), \tag{24}$$

$$\theta_1^{\pm} = \frac{(15+q)\pi}{8\eta(\eta \pm |\beta|)}, \tag{25}$$

$$\theta_2^{\pm}=\frac{1}{\eta^3(\eta\pm|\beta|)^4}\left\{\frac{64}{3}D^2\beta^8+D\left(\frac{1024}{3}D-128\right)\beta^6+\left(\frac{5056}{3}D^2-1024D+128\right)\beta^4\right.$$
$$+\left(\frac{8576}{3}D^2-2304D+768-\frac{225}{16}\pi^2\right)\beta^2+\frac{2560}{3}D^2-1024D+1024-\frac{675}{16}\pi^2$$
$$\left.+\left[\frac{16}{3}\beta^4+\left(32-\frac{15}{8}\pi^2\right)\beta^2+\frac{128}{3}-\frac{45}{8}\pi^2\right]q-\frac{\pi^2}{16}(\beta^2+3)q^2\right\}$$
$$\pm\frac{\eta|\beta|}{\eta^3(\eta\pm|\beta|)^4}\left[\frac{64}{3}D^2\beta^6+D\left(\frac{896}{3}D-128\right)\beta^4+\left(\frac{3392}{3}D^2-768D+128\right)\beta^2+\frac{3328}{3}D^2-1024D\right.$$
$$\left.+512-\frac{225}{16}\pi^2+\left(\frac{16}{3}\beta^2+\frac{64}{3}-\frac{15}{8}\pi^2\right)q-\frac{\pi^2}{16}q^2\right]. \tag{26}$$

They also satisfy the following relations:

$$\theta_0^+-\theta_0^-=|\beta|, \tag{27}$$

$$\theta_0^+\theta_0^-=1, \tag{28}$$

$$\theta_1^++\theta_1^-=\frac{15+q}{16}\pi, \tag{29}$$

$$\theta_1^+-\theta_1^-=-\frac{(15+q)\pi|\beta|}{16\eta}, \tag{30}$$

$$\theta_2^+-\theta_2^-=|\beta|\left[8D^2+\frac{225}{256}\pi^2-16\right.$$
$$\left.-\left(\frac{2}{3}-\frac{15}{128}\pi^2\right)q+\frac{\pi^2}{256}q^2\right]. \tag{31}$$

We can see that the black-bounce, traversable wormhole begins to differ from the Schwarzschild black hole starting from the next-to-leading-order term of the positions of the images.

### B. Magnifications

The magnification $\mu$ of a lensed image reads as [102]

$$\mu(\vartheta)=\left[\frac{\sin\mathcal{B}(\vartheta)}{\sin\vartheta}\frac{\mathrm{d}\mathcal{B}(\vartheta)}{\mathrm{d}\vartheta}\right]^{-1}, \tag{32}$$

and it can also be expanded into a series of $\varepsilon$ as

$$\mu=\mu_0+\varepsilon\mu_1+\varepsilon^2\mu_2+\mathcal{O}(\varepsilon^3). \tag{33}$$

Its zeroth-, first-, and second-order terms of the black-bounce, traversable wormhole can be obtained as

$$\mu_0=\frac{\theta_0^4}{\theta_0^4-1}, \tag{34}$$

$$\mu_1=-\frac{(15+q)\pi\theta_0^3}{16(\theta_0^2+1)^3}, \tag{35}$$

$$\mu_2=\frac{\theta_0^2}{(\theta_0^2+1)^5(\theta_0^2-1)}\left\{\frac{8}{3}D^2\theta_0^8+(48D^2-32D-32)\theta_0^6\right.$$
$$+\left(\frac{272}{3}D^2-64D+\frac{675}{128}\pi^2-64\right)\theta_0^4$$
$$+(48D^2-32D-32)\theta_0^2+\frac{8}{3}D^2$$
$$\left.-\left[\frac{4}{3}\theta_0^4+\left(\frac{8}{3}-\frac{45}{64}\pi^2\right)\theta_0^2+\frac{4}{3}\right]\theta_0^2q+\frac{3\pi^2}{128}\theta_0^4q^2\right\}, \tag{36}$$

and their values for the positive- and negative-parity images are

$$\mu_0^{\pm}=\frac{1}{2}\pm\frac{\beta^2+2}{2|\beta|\eta}, \tag{37}$$

$$\mu_1^+=\mu_1^-=-\frac{(15+q)\pi}{16\eta^3}, \tag{38}$$

$$\mu_2^{\pm}=\pm\frac{1}{|\beta|\eta^5}\left[\frac{8}{3}D^2\beta^4+\left(\frac{176}{3}D^2-32D-32\right)\beta^2\right.$$
$$-128D+192D^2+\frac{675}{128}\pi^2-128$$
$$\left.-\left(\frac{4}{3}\beta^2+\frac{16}{3}-\frac{45}{64}\pi^2\right)q+\frac{3\pi^2}{128}q^2\right], \tag{39}$$

leading to some neat relations

$$\mu_0^++\mu_0^-=1, \tag{40}$$

$$\mu_1^+-\mu_1^-=0, \tag{41}$$

$$\mu_2^++\mu_2^-=0, \tag{42}$$

and

$$\mu_0^+\theta_1^++\mu_0^-\theta_1^-+\mu_1^+\theta_0^++\mu_1^-\theta_0^-=0. \tag{43}$$

The leading terms of the magnifications are not affected by the black-bounce, traversable wormhole, with the same

values for the Schwarzschild black hole, while the next-to-leading-order terms explicitly depend on $q$ and go back to those of the Schwarzschild black hole as $q$ vanishes [43].

### C. Total magnification and centroid

When the two lensed images are blended, the total magnification and magnification-weighted centroid position will be the observables. The total magnification can be found as

$$\begin{aligned}\mu_{\rm tot} &= |\mu^+| + |\mu^-| \\ &= (2\mu_0^+ - 1) + 2\epsilon^2\mu_2^+ + \mathcal{O}(\varepsilon^3),\end{aligned} \tag{44}$$

where Eq. (41) is used. With the disappearance of the $\mathcal{O}(\varepsilon)$ contribution, the difference of the total magnification of the black-bounce, traversable wormhole from the one of the Schwarzschild black hole arises from the second-order approximation, demanding very high accuracy of photometry.

The magnification-weighted centroid position is given by

$$\Theta_{\rm cent} = \frac{\theta^+|\mu^+| - \theta^-|\mu^-|}{|\mu^+| + |\mu^-|}, \tag{45}$$

and can be expanded into

$$\Theta_{\rm cent} = \Theta_0 + \varepsilon\Theta_1 + \varepsilon^2\Theta_2 + \mathcal{O}(\varepsilon^3), \tag{46}$$

where

$$\Theta_0 = |\beta|\frac{\beta^2+3}{\beta^2+2}, \tag{47}$$

$$\Theta_1 = 0, \tag{48}$$

$$\begin{aligned}\Theta_2 = \frac{|\beta|}{\eta^2(\beta^2+2)^2}\Bigg[&\frac{8}{3}D^2\beta^6 + \left(\frac{104}{3}D - 16\right)D\beta^4 \\ &+ \left(\frac{272}{3}D^2 - 64D + 32\right)\beta^2 - \frac{64}{3}D^2 - \frac{675}{128}\pi^2 + 128 \\ &+ \left(\frac{4}{3}\beta^2 + \frac{16}{3} - \frac{45}{64}\pi^2\right)q - \frac{3\pi^2}{128}q^2\Bigg].\end{aligned} \tag{49}$$

The term $\Theta_1$ vanishes due to Eq. (41), while $\Theta_{\rm cent}$ of the black-bounce, traversable wormhole differs from the one of the Schwarzschild black hole starting from the second order, requiring high accuracy of astrometry on the centroid position.

### D. Differential time delay

The traveling time of a photon from the source to the observer reads as [100,103,104]

$$T = T(R_{\rm src}) + T(R_{\rm obs}), \tag{50}$$

with

$$T(R) = \int_{r_0}^{R}\left|\frac{{\rm d}t}{{\rm d}r}\right|{\rm d}r \tag{51}$$

and

$$\frac{{\rm d}t}{{\rm d}r} = \frac{\sqrt{B(r)C(r)A(r_0)}}{A(r)\sqrt{C(r_0)}\sqrt{\frac{C(r)}{C(r_0)}\frac{A(r_0)}{A(r)} - 1}}, \tag{52}$$

where $R_{\rm obs} = D_{\rm OL}$, and $R_{\rm src} = (D_{\rm OS}^2\tan^2\mathcal{B} + D_{\rm LS}^2)^{1/2}$ is the radial coordinate of the source with respect to the lens. The time delay is the difference between the light travel time with and without the lens and can be given as [43]

$$c\tau = T(R_{\rm src}) + T(R_{\rm obs}) - \frac{D_{\rm OS}}{\cos\mathcal{B}}. \tag{53}$$

The function $T(R)$ can be obtained as

$$T(R) = T_0 + \sum_{k=1}^{3}\frac{m_\bullet^k}{r_0^k}r_0T_k + \mathcal{O}\left(\frac{m_\bullet^4}{r_0^4}\right), \tag{54}$$

where

$$T_0 = \sqrt{R^2 - r_0^2}, \tag{55}$$

$$T_1 = \frac{\sqrt{1-\xi^2}}{\xi+1} + 2\ln\left(\frac{1+\sqrt{1-\xi^2}}{\xi}\right), \tag{56}$$

$$T_2 = \frac{15}{2}\arccos\xi - \left(2 + \frac{5}{2}\xi\right)\frac{\sqrt{1-\xi^2}}{(\xi+1)^2} + \frac{q}{2}\arccos\xi, \tag{57}$$

$$\begin{aligned}T_3 = &-\frac{15}{2}\arccos\xi + \frac{\sqrt{1-\xi^2}}{2(\xi+1)^3}(35\xi^3 + 133\xi^2 + 157\xi + 60) \\ &+ \left(\frac{\sqrt{1-\xi^2}}{\xi+1} - \frac{1}{2}\arccos\xi\right)q,\end{aligned} \tag{58}$$

with

$$\xi = \frac{r_0}{R}. \tag{59}$$

The term $T_0$ comes from the Euclidean geometry, while $T_1$ is the Shapiro delay, which is the same as the one for the Schwarzschild black hole [43]. The second- and higher-order terms are affected by the black-bounce, traversable wormhole.

We rescale the time delay of the lensed images $\tau$ as

$$\hat{\tau} = \frac{\tau}{\tau_{\rm E}}, \tag{60}$$

where

$$\tau_{\rm E} = 4m_{\bullet}, \tag{61}$$

so that it can be found as

$$\hat{\tau} = \hat{\tau}_0 + \varepsilon\hat{\tau}_1 + \mathcal{O}(\varepsilon^2), \tag{62}$$

where

$$\hat{\tau}_0 = \frac{1}{2}\left[1 + \beta^2 - \theta_0^2 - \ln\left(\frac{D_{\rm OL}\theta_0^2\vartheta_{\rm E}^2}{4D_{\rm LS}}\right)\right], \tag{63}$$

$$\hat{\tau}_1 = \frac{(15+q)\pi}{16\theta_0}. \tag{64}$$

Although the second-order term of the rescaled time delay could also be found, it is not as important as those of the image positions and magnification. The leading term of the time delay for the black-bounce, traversable wormhole has no difference from the one of the Schwarzschild black hole, and its next-to-leading-order term plays a role in distinguishing these two spacetime s. The differential time delay between the positive- and negative-parity images is given by

$$\Delta\hat{\tau} = \hat{\tau}_- - \hat{\tau}_+, \tag{65}$$

which can be expanded as

$$\Delta\hat{\tau} = \Delta\hat{\tau}_0 + \varepsilon\Delta\hat{\tau}_1 + \mathcal{O}(\varepsilon^2), \tag{66}$$

with

$$\Delta\hat{\tau}_0 = \frac{1}{2}\eta|\beta| + \ln\left(\frac{\eta + |\beta|}{\eta - |\beta|}\right), \tag{67}$$

$$\Delta\hat{\tau}_1 = \frac{15+q}{16}\pi|\beta|. \tag{68}$$

If the first-order correction to the differential time delay between the two lensed images could be measured, it might be used to test the black-bounce, traversable wormhole.

### E. Practical observables

Practical observables for the weak deflection gravitational lensing by the black-bounce, traversable wormhole can be constructed by the aforementioned quantities and their relations, in which the physical quantities $(\mathcal{B}, \vartheta, F, \tau)$ are obtained from the rescaled ones $(\beta, \theta, \mu, \hat{\tau})$. The observed flux of the light $F$ is proportional to the unlensed flux of the source $F_{\rm src}$ by a factor of the absolute magnification $|\mu|$. The practical observables contain the positions, magnitudes of brightness, centroid, and differential time delay between the lensed images, and they are [43,44]

$$P_{\rm tot} \equiv \vartheta^+ + \vartheta^- = \mathcal{E} + \frac{15+q}{16}\varepsilon\pi\vartheta_{\rm E} + \mathcal{O}(\varepsilon^2), \tag{69}$$

$$\Delta P \equiv \vartheta^+ - \vartheta^- = |\mathcal{B}|\left(1 - \frac{15+q}{16}\varepsilon\pi\frac{\vartheta_{\rm E}}{\mathcal{E}}\right) + \mathcal{O}(\varepsilon^2), \tag{70}$$

$$F_{\rm tot} \equiv F^+ + F^- = F_{\rm src}\frac{\mathcal{B}^2 + 2\vartheta_{\rm E}^2}{|\mathcal{B}|\mathcal{E}} + \mathcal{O}(\varepsilon^2), \tag{71}$$

$$\Delta F \equiv F^+ - F^- = F_{\rm src} - F_{\rm src}\frac{15+q}{8}\varepsilon\pi\frac{\vartheta_{\rm E}^3}{\mathcal{E}^3} + \mathcal{O}(\varepsilon^2), \tag{72}$$

$$S_{\rm cent} \equiv \frac{\vartheta^+F^+ - \vartheta^-F^-}{F_{\rm tot}} = |\mathcal{B}|\frac{\mathcal{B}^2 + 3\vartheta_{\rm E}^2}{\mathcal{B}^2 + 2\vartheta_{\rm E}^2} + \mathcal{O}(\varepsilon^2), \tag{73}$$

$$\Delta\tau = \frac{D_{\rm OL}D_{\rm OS}}{cD_{\rm LS}}\left\{\frac{1}{2}|\mathcal{B}|\mathcal{E} + \vartheta_{\rm E}^2\ln\left(\frac{\mathcal{E} + |\mathcal{B}|}{\mathcal{E} - |\mathcal{B}|}\right) + \varepsilon\frac{15+q}{16}\pi\vartheta_{\rm E}|\mathcal{B}| + \mathcal{O}(\varepsilon^2)\right\}, \tag{74}$$

where

$$\mathcal{E} = \sqrt{\mathcal{B}^2 + 4\vartheta_{\rm E}^2}. \tag{75}$$

We ignore the $\mathcal{O}(\varepsilon^2)$ corrections in the practical observables since they are far beyond the capability of current technology. The total flux $F_{\rm tot}$ and the centroid $S_{\rm cent}$ merely have their leading-order terms, which are indistinguishable from those of the Schwarzschild black hole, because their first-order corrections cancel out exactly.

We define the following indicators to demonstrate the deviations of these observables from those of the Schwarzschild black hole, which are

$$\delta P_{\rm tot} \equiv P_{\rm tot} - P_{\rm tot}(q=0) = \frac{q}{16}\varepsilon\pi\vartheta_{\rm E} + \mathcal{O}(\varepsilon^2), \tag{76}$$

$$\delta\Delta P \equiv \Delta P - \Delta P(q=0) = -\frac{q}{16}\varepsilon\pi|\mathcal{B}|\frac{\vartheta_{\rm E}}{\mathcal{E}} + \mathcal{O}(\varepsilon^2), \tag{77}$$

$$\delta r_{\rm tot} \equiv 2.5\log_{10}\left[\frac{F_{\rm tot}}{F_{\rm tot}(q=0)}\right] = \mathcal{O}(\varepsilon^2), \tag{78}$$

$$\delta\Delta r \equiv 2.5\log_{10}\left[\frac{\Delta F}{\Delta F(q=0)}\right] = -\frac{5}{16\log 10}q\varepsilon\pi\frac{\vartheta_{\rm E}^3}{\mathcal{E}^3} + \mathcal{O}(\varepsilon^2), \tag{79}$$

$$\delta S_{\rm cent} \equiv F_{\rm cent} - F_{\rm cent}(q=0) = \mathcal{O}(\varepsilon^2), \tag{80}$$

$$\delta\Delta\tau \equiv \Delta\tau - \Delta\tau(q=0) = \frac{D_{\rm OL}D_{\rm OS}}{16cD_{\rm LS}}\varepsilon q\pi\vartheta_{\rm E}|\mathcal{B}| + \mathcal{O}(\varepsilon^2), \tag{81}$$

where the fluxes are converted to the magnitudes for astronomical conventions. $P_{\rm tot}$, $\Delta P$, $\Delta r$, and $\Delta\tau$ and their deviations from those of the Schwarzschild black hole $\delta P_{\rm tot}$, $\delta\Delta P$, $\delta\Delta r$, and $\delta\Delta\tau$ have $\mathcal{O}(\varepsilon)$ contributions, which might be measured in the future. In the next section, they will be estimated for various scenarios on the domain

$$\mathcal{D} = \{(q,\beta)|0 < q < 9, 10^{-2} < \beta < 10\}. \tag{82}$$

On the other hand, $\delta r_{\rm tot}$ and $\delta S_{\rm cent}$ are of the order of $\mathcal{O}(\varepsilon^2)$, making them hard to access in the foreseeable future.

## IV. SCENARIOS OF LENSING

### A. Sgr A*

The Galactic Center remains a unique place where we can directly observe stars orbiting the supermassive black hole, Sgr A*. We take it as the lens with $m_\bullet = 4.28 \times 10^6\ M_\odot$ and $D_{\rm OL} = 8.32$ kpc [105]. Based on the fact that the star S175 orbiting Sgr A* has the periastron distance of $2 \times 10^{-4}$ pc [105], we assume a luminous object surrounding Sgr A* with a distance $D_{\rm LS} = 10^{-3}$ pc. For such a source, its angular Einstein radius is $\theta_{\rm E} = 710\ \mu$as, and its small parameter is $\varepsilon = 7.2 \times 10^{-3}$ where the condition $D_{\rm OS} \approx D_{\rm OL}$ is used. In this scenario of the weak deflection gravitational lensing, we have four practical observables $P_{\rm tot}$, $\Delta P$, $\Delta F$, and $\Delta\tau$ and their deviations from those of the Schwarzschild black hole of the order of $\mathcal{O}(\varepsilon)$.

The left column of Fig. 1 shows color indexed $P_{\rm tot}$, $\Delta P$, $\Delta F$, and $\Delta\tau$ from top to bottom, and its right column shows their deviations from those of the Schwarzschild black hole, i.e., $\delta P_{\rm tot}$, $\delta\Delta P$, $\delta\Delta r$, and $\delta\Delta\tau$. In this figure, the dash-dotted line marks the best estimated value of $q$ based on the shadow of M87* observed by EHT, and the dotted lines denote its $1\sigma$ uncertainties.

The angular separation between the two images $P_{\rm tot}$ ranges from about 2 to 7 milliarcsecond (mas), and it barely changes with respect to $q$. Since GRAVITY has the extremely high angular resolution of about 3 mas at $K$ band (1.95–2.45 $\mu$m) [71], it would be feasible to resolve these images in the best conditions. The deviation of $P_{\rm tot}$ from the one of the Schwarzschild black hole $\delta P_{\rm tot}$ strongly depends on $q$. For a $q \in \mathcal{D}_{\rm EHT}$, $\delta P_{\rm tot}$ can range from about 13 to 22 $\mu$as, which would be marginally detected by very accurate astrometry of GRAVITY with errors as low as 10–20 $\mu$as [71,72]. The angular difference between the two lensed images $\Delta P$ is almost immune to $q$ and changes from about 0.5 to 6.8 mas, within reach of the current best ability of GRAVITY. When $\beta$ is between 1 to 10 and $q$ belongs to $\mathcal{D}_{\rm EHT}$, its deviation from the one of the Schwarzschild black hole $\delta\Delta P$ varies distinctly from about $-22$ to $-10\ \mu$as which would be narrowly within the capability of GRAVITY [71,72], otherwise, $\delta\Delta P$ nearly vanishes. The normalized fluxes difference $\Delta F/F_{\rm src}$ can reach about 0.987 when $\beta < 0.1$ and $q \in \mathcal{D}_{\rm EHT}$. In this situation, its deviation from the one of the Schwarzschild black hole $\delta\Delta r$ is about $-8.5 \times 10^{-3}$ mag. Such a $\delta\Delta r$ might be distinguished by a dedicated space telescope, such as the one with photometry ability like the Transiting Exoplanet Survey Satellite [106], but observations have to wait for a quiescent state of Sgr A*, otherwise flares of Sgr A* and their motions, typically a few times per day and lasting for about 1–2 h [107–109], might overwhelm this brightness difference. The differential time delay between the two lensed images $\Delta\tau$ varies from about 10 to 70 min, and its deviation from the Schwarzschild black hole's $\delta\Delta\tau$ is about 15–25 s when $\beta \approx 10$ and $q \in \mathcal{D}_{\rm EHT}$. Both of them might be detected by GRAVITY since its typical dataset of Sgr A* and S2 contains 30 exposures with an individual integration time of 10 s.

To summarize the weak deflection gravitational lensing by Sgr A*, we find that (1) the angular separation $P_{\rm tot}$, the angular difference $\Delta P$, the fluxes difference $\Delta F$, and the time delay $\Delta\tau$ are potentially feasible to detect by current techniques, and (2) the black-bounce, traversable wormhole currently might be able to be marginally tested by measuring its deviations from these observables of the Schwarzschild black hole for $q \in \mathcal{D}_{\rm EHT}$, either with $\delta P_{\rm tot}$, $\delta\Delta P$, and $\delta\Delta\tau$ by GRAVITY or with $\delta\Delta r$ by a dedicated space telescope. We expect that these tests would become more robust with further improvements of GRAVITY.

### B. A microlensed bulge star

In the scenario of microlensing, a more distant background star is lensed by a foreground gravitational object. Some projects [110–115] have been monitoring the brightness change of stars in the Galactic bulge by microlensing of an object in the Galactic disk.

We take the black-bounce, traversable wormhole as the lens with $m_\bullet = M_\odot$ and $D_{\rm OL} = 4$ kpc and assume a bright star in the bulge with $D_{\rm OS} = 8$ kpc so that $\vartheta_\bullet \sim 2.5$ picoarcsecond (pas), $\vartheta_{\rm E} \sim 1$ mas, and $\varepsilon \sim 2.4 \times 10^{-9}$. It is also supposed that the black-bounce, traversable wormhole is isolated, and it would be a dark lens without any emission by accretion. Although the total flux $F_{\rm tot}$ is usually the most significant observable, it is identical to that of the Schwarzschild black hole at the leading- and next-to-leading-order approximations as we show in Sec. III E. Therefore, we focus on the observables that can distinguish the black-bounce, traversable wormhole from the Schwarzschild black hole, such as the angular separation $P_{\rm tot}$ and the fluxes difference $\Delta F$ between the two images.

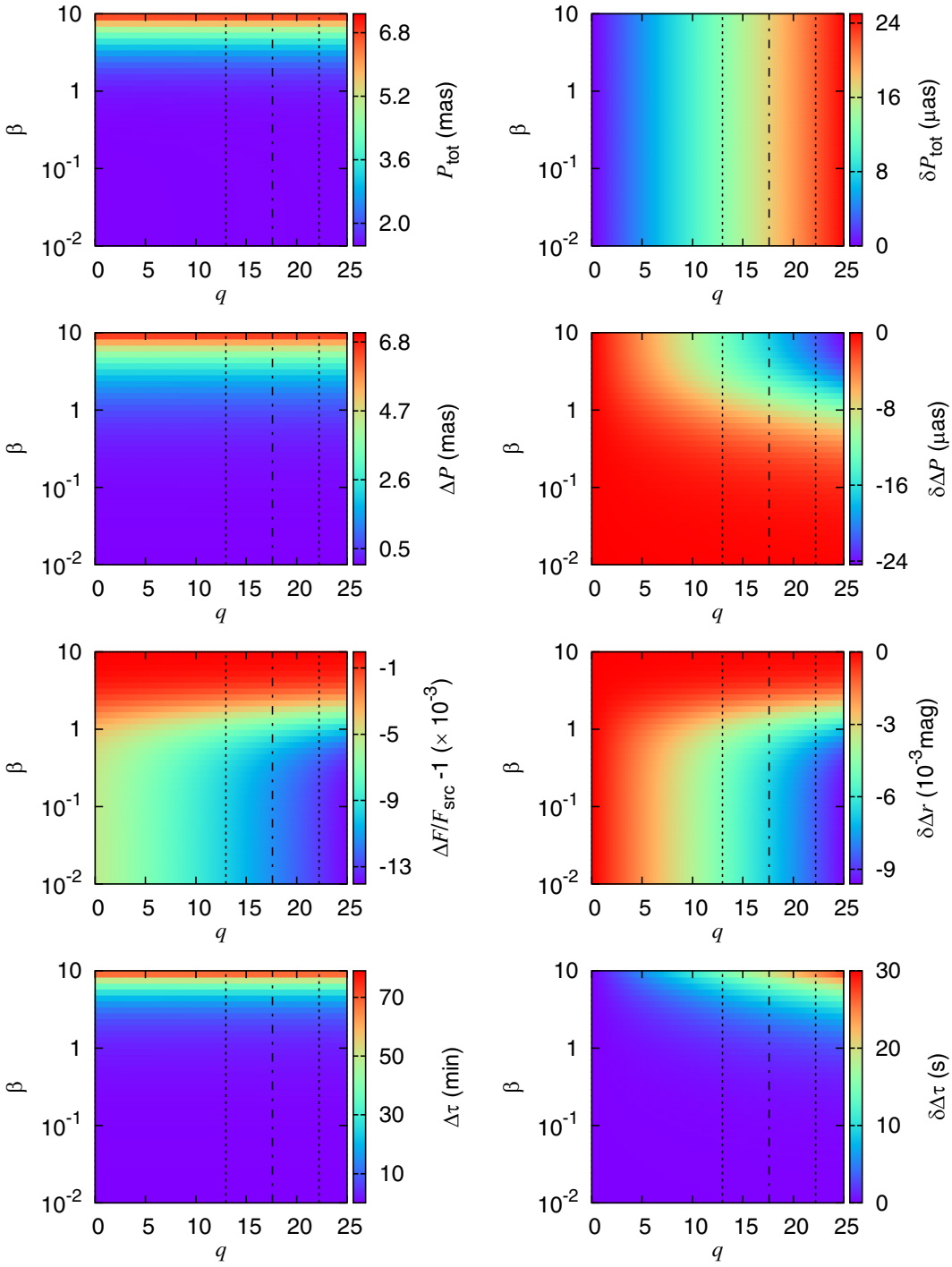


FIG. 1. Color-indexed practical observables in the weak deflection gravitational lensing by the black-bounce, traversable wormhole for Sgr A* and their deviations from those of the Schwarzschild black hole. From top to bottom: $P_{tot}$, $\Delta P$, $\Delta F$, and $\Delta\tau$ are shown in the left column, and $\delta P_{tot}$, $\delta\Delta P$, $\delta\Delta r$, and $\delta\Delta\tau$ are given in the right column. The dash-dotted line marks the best estimated value of $q$ based on the shadow of M87* observed by EHT and the dotted lines denote its $1\sigma$ uncertainties.

Figure 2 shows color-indexed $P_{tot}$ and $\Delta F$ in the left column and their deviations from those of the Schwarzschild black hole in the right column where the dash-dotted line marks the best estimated value of $q$ based on the M87*'s shadow and the dotted lines denote its uncertainties. Although $P_{tot}$ ranges from about 2 to 10 mas, resolvable with current ability, its deviation $\delta P_{tot}$ is only about 12 pas at best, far beyond the territory of foreseeable techniques. Meanwhile, both the brightness difference and its deviation are too small to detect.

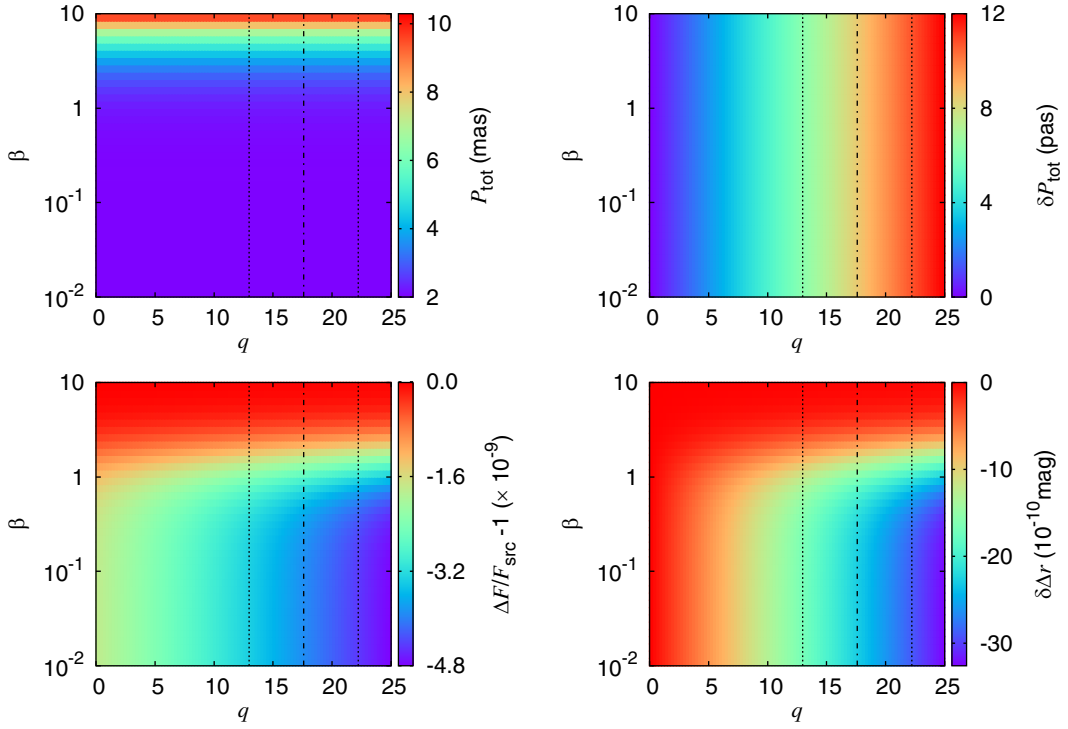


FIG. 2. Color-indexed observables and their deviations from those of the Schwarzschild black hole for the weak deflection gravitational lensing by the black-bounce, traversable wormhole on a star in the Galactic bulge. From top to bottom: $P_{\rm tot}$ and $\Delta F$ are shown in the left column, and their deviations $\delta P_{\rm tot}$ and $\delta\Delta r$ are given in the right column. The dash-dotted line marks the best estimated value of $q$ based on the shadow of M87* observed by EHT and the dotted lines denote its $1\sigma$ uncertainties.

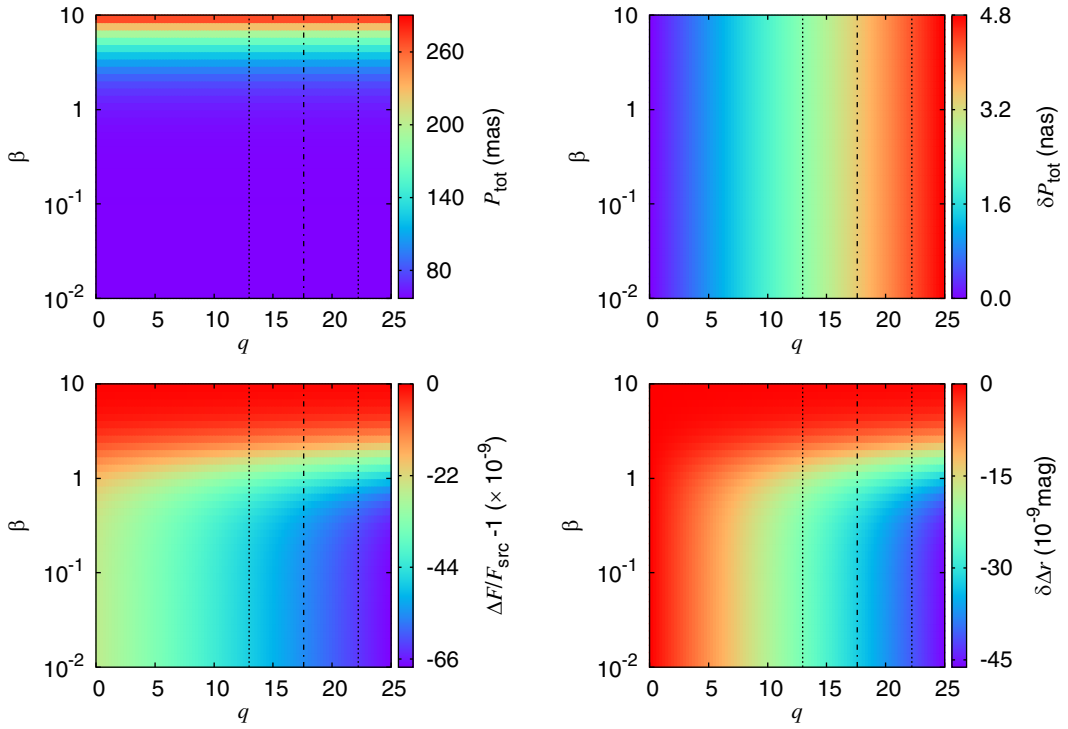


FIG. 3. Color-indexed observables and their deviations from those of the Schwarzschild black hole for the weak deflection gravitational lensing by a nearby black-bounce, traversable wormhole. From top to bottom: $P_{\rm tot}$ and $\Delta F$ are shown in the left column, and their deviations $\delta P_{\rm tot}$ and $\delta\Delta r$ are given in the right column. The dash-dotted line marks the best estimated value of $q$ based on the shadow of M87* observed by EHT and the dotted lines denote its $1\sigma$ uncertainties.

In summary, it is presently possible to separate the two images of a bulge star in the microlensing by the black-bounce, traversable wormhole, while it is impossible to distinguish it from the Schwarzschild black hole by the lensing observables.

### C. Microlensing by a nearby lens

In the microlensing, the lens could also be a nearby object within ∼10 pc, which has been widely studied [116–118] and routinely observed [42,119,120].

We assume a source with distance $D_{\rm OS} = 2$ kpc and a nearby black-bounce, traversable wormhole as the lens with $m_\bullet = M_\odot$ located at $D_{\rm OL} = 10$ pc from the observer, leading to $\vartheta_\bullet \sim 1$ nanoarcsecond (nas), $\vartheta_{\rm E} \sim 29$ mas, and $\varepsilon \sim 3.5 \times 10^{-8}$. Such an Einstein ring radius is nearly 30 times larger than that of the microlensing on a Galactic bulge star.

In practice, $P_{\rm tot}$ and $\Delta F$ can be observed and used to tell the difference between the black-bounce, traversable wormhole and the Schwarzschild black hole. They are shown in the left column of Fig. 3, and their deviations from those of the Schwarzschild black hole are given in the right column. In this case, $P_{\rm tot}$ can reach about 260 mas, totally accessible with current capability, whereas its deviation $\delta P_{\rm tot}$ is no more than 5 nas, impossible to measure for now and in the foreseeable future. In addition, it is unfeasible to detect the brightness difference and its deviation.

In summary, it is able to resolve the two images of the weak deflection gravitational lensing by the nearby black bounce, traversable wormhole, but distinguishing it from the Schwarzschild black hole through its lensing observables is still beyond the reach of current ability.

## V. CONCLUSIONS AND DISCUSSION

In the strong deflection gravitational lensing, considering the facts that the black-bounce, traversable wormhole is indistinguishable from the Schwarzschild black hole by observing its shadow and relativistic images [31] and it is just loosely constrained [32] but cannot currently be tested by the observation of EHT [34], we investigate its signatures in the weak deflection gravitational lensing to provide some clues about it in light of the tremendous progress made by the near-infrared interferometer GRAVITY. We obtain its bending angle, image positions, magnifications, centroid, and time delay and find its practical observables and their deviations from those of the Schwarzschild black hole. The lensing effects are studied for three specific astrophysical scenarios: an orbiting star lensed by Sgr A*, a microlensed star in the Galactic bulge, and microlensing by a nearby lens. We find that the measurements of the observables in the weak deflection gravitational lensing by Sgr A* provide a promising way to test the black-bounce, traversable wormhole spacetime with $q \in \mathcal{D}_{\rm EHT}$. GRAVITY can resolve the angular separation $P_{\rm tot}$, the angular difference $\Delta P$, and the time delay $\Delta\tau$, and it can marginally detect their deviations from these observables of the Schwarzschild black hole $\delta P_{\rm tot}$, $\delta\Delta P$, and $\delta\Delta\tau$. The fluxes difference $\Delta F$ and its deviation $\delta\Delta r$ might be measured by a dedicated space telescope. In the near future, we expect that the black-bounce, traversable wormhole would be more robustly tested with the weak deflection gravitational lensing by further improved and upgraded GRAVITY+. Therefore, it might also be possible to distinguish wormholes from black holes by stacking the data from several wormholes or black holes.

In this work, a static black-bounce, traversable wormhole without spinning is considered. However, in the real Universe, the black-bounce, traversable wormhole could rotate and move with some speed. These properties would change its signatures of the weak deflection gravitational lensing, making it more complicated by causing the caustic to be shifted and distorted [121–137]. Besides the time delay, other kinds of time-domain signals [138–143] might provide useful information about it as well. Meanwhile, timelike geodesics around the black-bounce, traversable wormhole is another important aspect in order to understand its features. Precessing [144–149] and periodic [150–158] orbits might also provide insights into such a spacetime.

## ACKNOWLEDGMENTS

We are very grateful to our anonymous referees who helped significantly to improve this paper. This work is funded by the National Natural Science Foundation of China (Grants No. 11573015 and No. 11833004) and the Strategic Priority Research Program of Chinese Academy of Sciences (Grant No. XDA15016700).

[1] B. P. Abbott *et al.* (LIGO Scientific and Virgo Collaborations), Phys. Rev. Lett. **116**, 061102 (2016).
[2] B. P. Abbott *et al.* (LIGO Scientific and Virgo Collaborations), Phys. Rev. X **6**, 041015 (2016).
[3] B. P. Abbott *et al.* (LIGO Scientific and Virgo Collaborations), Phys. Rev. Lett. **116**, 241103 (2016).
[4] B. P. Abbott *et al.* (LIGO Scientific and Virgo Collaborations), Phys. Rev. Lett. **118**, 221101 (2017).
[5] B. P. Abbott *et al.* (LIGO Scientific and Virgo Collaborations), Astrophys. J. Lett. **851**, L35 (2017).
[6] B. P. Abbott *et al.* (LIGO Scientific and Virgo Collaborations), Phys. Rev. Lett. **119**, 141101 (2017).

[7] K. Akiyama *et al.* (Event Horizon Telescope Collaboration), Astrophys. J. Lett. **875**, L1 (2019).
[8] K. Akiyama *et al.* (Event Horizon Telescope Collaboration), Astrophys. J. Lett. **875**, L2 (2019).
[9] K. Akiyama *et al.* (Event Horizon Telescope Collaboration), Astrophys. J. Lett. **875**, L3 (2019).
[10] K. Akiyama *et al.* (Event Horizon Telescope Collaboration), Astrophys. J. Lett. **875**, L4 (2019).
[11] K. Akiyama *et al.* (Event Horizon Telescope Collaboration), Astrophys. J. Lett. **875**, L5 (2019).
[12] K. Akiyama *et al.* (Event Horizon Telescope Collaboration), Astrophys. J. Lett. **875**, L6 (2019).
[13] J. Bardeen, in *Proceedings of International Conference GR5* (Tbilisi University Press, Tbilisi, USSR, 1968), p. 174.
[14] S. A. Hayward, Phys. Rev. Lett. **96**, 031103 (2006).
[15] C. Bejarano, G. J. Olmo, and D. Rubiera-Garcia, Phys. Rev. D **95**, 064043 (2017).
[16] C. C. Menchon, G. J. Olmo, and D. Rubiera-Garcia, Phys. Rev. D **96**, 104028 (2017).
[17] V. P. Frolov and G. A. Vilkovisky, Phys. Lett. **106B**, 307 (1981).
[18] M. Ambrus and P. Hájíček, Phys. Rev. D **72**, 064025 (2005).
[19] C. Barceló, R. Carballo-Rubio, L. J. Garay, and G. Jannes, Classical Quantum Gravity **32**, 035012 (2015).
[20] C. Barceló, S. Liberati, S. Sonego, and M. Visser, Phys. Rev. D **77**, 044032 (2008).
[21] S. D. Mathur, Classical Quantum Gravity **26**, 224001 (2009).
[22] S. D. Mathur and D. Turton, J. High Energy Phys. 01 (2014) 034.
[23] B. Guo, S. Hampton, and S. D. Mathur, J. High Energy Phys. 07 (2018) 162.
[24] R. Carballo-Rubio, F. Di Filippo, S. Liberati, and M. Visser, Phys. Rev. D **98**, 124009 (2018).
[25] A. Simpson and M. Visser, J. Cosmol. Astropart. Phys. 02 (2019) 042.
[26] H. G. Ellis, J. Math. Phys. (N.Y.) **14**, 104 (1973).
[27] A. Simpson, P. Martín-Moruno, and M. Visser, Classical Quantum Gravity **36**, 145007 (2019).
[28] F. S. N. Lobo, A. Simpson, and M. Visser, Phys. Rev. D **101**, 124035 (2020).
[29] M. S. Churilova and Z. Stuchlík, Classical Quantum Gravity **37**, 075014 (2020).
[30] H. C. D. L. Junior, C. L. Benone, and L. C. B. Crispino, Phys. Rev. D **101**, 124009 (2020).
[31] J. R. Nascimento, A. Y. Petrov, P. J. Porfírio, and A. R. Soares, Phys. Rev. D **102**, 044021 (2020).
[32] N. Tsukamoto, Phys. Rev. D **103**, 024033 (2021).
[33] D. Psaltis *et al.* (Event Horizon Telescope Collaboration), Phys. Rev. Lett. **125**, 141104 (2020).
[34] S. E. Gralla, Phys. Rev. D **103**, 024023 (2021).
[35] S. E. Gralla, D. E. Holz, and R. M. Wald, Phys. Rev. D **100**, 024018 (2019).
[36] M. D. Johnson, A. Lupsasca, A. Strominger, G. N. Wong, S. Hadar, D. Kapec, R. Narayan, A. Chael, C. F. Gammie, P. Galison, D. C. M. Palumbo, S. S. Doeleman, L. Blackburn, M. Wielgus, D. W. Pesce, J. R. Farah, and J. M. Moran, Sci. Adv. **6**, eaaz1310 (2020).
[37] S. E. Gralla and A. Lupsasca, Phys. Rev. D **102**, 124003 (2020).
[38] S. E. Gralla, A. Lupsasca, and D. P. Marrone, Phys. Rev. D **102**, 124004 (2020).
[39] P. Schneider, J. Ehlers, and E. E. Falco, *Gravitational Lenses* (Springer-Verlag, Berlin, 1992).
[40] A. O. Petters, H. Levine, and J. Wambsganss, *Singularity Theory and Gravitational Lensing* (Birkhäuser, Boston, 2001).
[41] P. Schneider, C. S. Kochanek, and J. Wambsganss, in *Saas-Fee Advanced Course 33: Gravitational Lensing: Strong, Weak and Micro*, edited by G. Meylan, P. Jetzer, and P. North (Springer-Verlag, Berlin, 2006).
[42] K. C. Sahu, J. Anderson, S. Casertano, H. E. Bond, P. Bergeron, E. P. Nelan, L. Pueyo, T. M. Brown, A. Bellini, Z. G. Levay, J. Sokol, aff1, M. Dominik, A. Calamida, N. Kains, and M. Livio, Science **356**, 1046 (2017).
[43] C. R. Keeton and A. O. Petters, Phys. Rev. D **72**, 104006 (2005).
[44] C. R. Keeton and A. O. Petters, Phys. Rev. D **73**, 044024 (2006).
[45] C. R. Keeton and A. O. Petters, Phys. Rev. D **73**, 104032 (2006).
[46] G. Li and X.-M. Deng, Ann. Phys. (Amsterdam) **382**, 136 (2017).
[47] T. E. Collett, L. J. Oldham, R. J. Smith, M. W. Auger, K. B. Westfall, D. Bacon, R. C. Nichol, K. L. Masters, K. Koyama, and R. van den Bosch, Science **360**, 1342 (2018).
[48] Y. Xie, Phys. Rev. D **98**, 021501(R) (2018).
[49] F. Abe, Astrophys. J. **725**, 787 (2010).
[50] Y. Toki, T. Kitamura, H. Asada, and F. Abe, Astrophys. J. **740**, 121 (2011).
[51] K. Nakajima and H. Asada, Phys. Rev. D **85**, 107501 (2012).
[52] T. Kitamura, K. Nakajima, and H. Asada, Phys. Rev. D **87**, 027501 (2013).
[53] K. Izumi, C. Hagiwara, K. Nakajima, T. Kitamura, and H. Asada, Phys. Rev. D **88**, 024049 (2013).
[54] T. Kitamura, K. Izumi, K. Nakajima, C. Hagiwara, and H. Asada, Phys. Rev. D **89**, 084020 (2014).
[55] K. Nakajima, K. Izumi, and H. Asada, Phys. Rev. D **90**, 084026 (2014).
[56] N. Tsukamoto and Y. Gong, Phys. Rev. D **97**, 084051 (2018).
[57] M. Safonova, D. F. Torres, and G. E. Romero, Phys. Rev. D **65**, 023001 (2001).
[58] R. Shaikh and S. Kar, Phys. Rev. D **96**, 044037 (2017).
[59] R. F. Lukmanova, G. Y. Tuleganova, R. N. Izmailov, and K. K. Nandi, Phys. Rev. D **97**, 124027 (2018).
[60] Z. Horváth, L. Á. Gergely, Z. Keresztes, T. Harko, and F. S. N. Lobo, Phys. Rev. D **84**, 083006 (2011).
[61] E. F. Eiroa and C. M. Sendra, Phys. Rev. D **86**, 083009 (2012).
[62] E. F. Eiroa and C. M. Sendra, Phys. Rev. D **88**, 103007 (2013).
[63] C.-Y. Wang, Y.-F. Shen, and Y. Xie, J. Cosmol. Astropart. Phys. 04 (2019) 022.
[64] R. N. Izmailov, R. K. Karimov, E. R. Zhdanov, and K. K. Nandi, Mon. Not. R. Astron. Soc. **483**, 3754 (2019).
[65] F.-Y. Liu, Y.-F. Mai, W.-Y. Wu, and Y. Xie, Phys. Lett. B **795**, 475 (2019).

[66] X. Pang and J. Jia, Classical Quantum Gravity **36**, 065012 (2019).
[67] X. Lu and Y. Xie, Eur. Phys. J. C **79**, 1016 (2019).
[68] X. Lu and Y. Xie, Mod. Phys. Lett. A **34**, 1950152 (2019).
[69] X. Lu and Y. Xie, Eur. Phys. J. C **80**, 625 (2020).
[70] Y.-X. Gao and Y. Xie, Phys. Rev. D **103**, 043008 (2021).
[71] R. Abuter *et al.* (GRAVITY Collaboration), Astron. Astrophys. **602**, A94 (2017).
[72] R. Abuter *et al.* (GRAVITY Collaboration), Astron. Astrophys. **625**, L10 (2019).
[73] R. Abuter *et al.* (GRAVITY Collaboration), Astron. Astrophys. **615**, L15 (2018).
[74] R. Abuter *et al.* (GRAVITY Collaboration), Astron. Astrophys. **636**, L5 (2020).
[75] R. Abuter *et al.* (GRAVITY Collaboration), arXiv: 2101.12098.
[76] R. Abuter *et al.* (GRAVITY Collaboration), Astron. Astrophys. **645**, A127 (2021).
[77] N. Tsukamoto, T. Harada, and K. Yajima, Phys. Rev. D **86**, 104062 (2012).
[78] N. Tsukamoto, Phys. Rev. D **94**, 124001 (2016).
[79] N. Tsukamoto and T. Harada, Phys. Rev. D **95**, 024030 (2017).
[80] R. Takahashi and H. Asada, Astrophys. J. Lett. **768**, L16 (2013).
[81] V. Cardoso and P. Pani, Living Rev. Relativity **22**, 4 (2019).
[82] J. G. Cramer, R. L. Forward, M. S. Morris, M. Visser, G. Benford, and G. A. Landis, Phys. Rev. D **51**, 3117 (1995).
[83] K. K. Nandi, Y.-Z. Zhang, and A. V. Zakharov, Phys. Rev. D **74**, 024020 (2006).
[84] C. Bambi, Phys. Rev. D **87**, 107501 (2013).
[85] K. K. Nandi, R. N. Izmailov, E. R. Zhdanov, and A. Bhattacharya, J. Cosmol. Astropart. Phys. 07 (2018) 027.
[86] K. Jusufi, N. Sarkar, F. Rahaman, A. Banerjee, and S. Hansraj, Eur. Phys. J. C **78**, 349 (2018).
[87] K. Jusufi and A. Övgün, Phys. Rev. D **97**, 024042 (2018).
[88] R. Shaikh, Phys. Rev. D **98**, 024044 (2018).
[89] R. Shaikh, P. Banerjee, S. Paul, and T. Sarkar, Phys. Lett. B **789**, 270 (2019).
[90] R. Shaikh, P. Banerjee, S. Paul, and T. Sarkar, J. Cosmol. Astropart. Phys. 07 (2019) 028.
[91] M. Amir, K. Jusufi, A. Banerjee, and S. Hansraj, Classical Quantum Gravity **36**, 215007 (2019).
[92] S. Sahu, M. Patil, D. Narasimha, and P. S. Joshi, Phys. Rev. D **86**, 063010 (2012).
[93] R. Shaikh, P. Kocherlakota, R. Narayan, and P. S. Joshi, Mon. Not. R. Astron. Soc. **482**, 52 (2019).
[94] T. Kubo and N. Sakai, Phys. Rev. D **93**, 084051 (2016).
[95] P. V. P. Cunha, J. A. Font, C. Herdeiro, E. Radu, N. Sanchis-Gual, and M. Zilhão, Phys. Rev. D **96**, 104040 (2017).
[96] M. Patil, P. Mishra, and D. Narasimha, Phys. Rev. D **95**, 024026 (2017).
[97] R. Shaikh, P. Banerjee, S. Paul, and T. Sarkar, Phys. Rev. D **99**, 104040 (2019).
[98] X.-Y. Zhu and Y. Xie, Eur. Phys. J. C **80**, 444 (2020).
[99] K. S. Virbhadra, D. Narasimha, and S. M. Chitre, Astron. Astrophys. **337**, 1 (1998), https://ui.adsabs.harvard.edu/abs/1998A%26A...337....1V/abstract.
[100] S. Weinberg, *Gravitation and Cosmology: Principles and Applications of the General Theory of Relativity* (Wiley, New York, 1972).
[101] K. S. Virbhadra and G. F. R. Ellis, Phys. Rev. D **62**, 084003 (2000).
[102] S. Refsdal, Mon. Not. R. Astron. Soc. **128**, 295 (1964).
[103] V. Bozza and L. Mancini, Gen. Relativ. Gravit. **36**, 435 (2004).
[104] K. S. Virbhadra and C. R. Keeton, Phys. Rev. D **77**, 124014 (2008).
[105] S. Gillessen, P. M. Plewa, F. Eisenhauer, R. Sari *et al.*, Astrophys. J. **837**, 30 (2017).
[106] C. X. Huang *et al.*, Astrophys. J. Lett. **868**, L39 (2018).
[107] F. Eisenhauer *et al.*, Astrophys. J. **628**, 246 (2005).
[108] G. Witzel, G. Martinez, J. Hora, S. P. Willner, M. R. Morris, C. Gammie, E. E. Becklin, M. L. N. Ashby, F. Baganoff, S. Carey, T. Do, G. G. Fazio, A. Ghez, W. J. Glaccum, D. Haggard, R. Herrero-Illana, J. Ingalls, R. Narayan, and H. A. Smith, Astrophys. J. **863**, 15 (2018).
[109] R. Abuter *et al.* (GRAVITY Collaboration), Astron. Astrophys. **618**, L10 (2018).
[110] C. Alcock, C. W. Akerlof, R. A. Allsman, T. S. Axelrod, D. P. Bennett, S. Chan, K. H. Cook, K. C. Freeman, K. Griest, S. L. Marshall, H.-S. Park, S. Perlmutter, B. A. Peterson, M. R. Pratt, P. J. Quinn, A. W. Rodgers, C. W. Stubbs, and W. Sutherland, Nature (London) **365**, 621 (1993).
[111] A. Udalski, M. Szymanski, J. Kaluzny, M. Kubiak, W. Krzeminski, M. Mateo, G. W. Preston, and B. Paczynski, Acta Astron. **43**, 289 (1993), https://ui.adsabs.harvard.edu/abs/1993AcA....43..289U/abstract.
[112] E. Aubourg *et al.*, Nature (London) **365**, 623 (1993).
[113] C. Alard, J. Guibert, O. Bienayme, D. Valls-Gabaud, A. C. Robin, A. Terzan, and E. Bertin, Messenger **80**, 31 (1995), https://ui.adsabs.harvard.edu/abs/1995Msngr..80...31A/abstract.
[114] I. A. Bond *et al.*, Mon. Not. R. Astron. Soc. **327**, 868 (2001).
[115] M. G. Navarro, D. Minniti, and R. Contreras Ramos, Astrophys. J. Lett. **851**, L13 (2017).
[116] M. A. Walker, Astrophys. J. **453**, 37 (1995).
[117] M. Dominik and K. C. Sahu, Astrophys. J. **534**, 213 (2000).
[118] S. Proft, M. Demleitner, and J. Wambsganss, Astron. Astrophys. **536**, A50 (2011).
[119] K. C. Sahu, H. E. Bond, J. Anderson, and M. Dominik, Astrophys. J. **782**, 89 (2014).
[120] N. Kains, A. Calamida, K. C. Sahu, S. Casertano, J. Anderson, A. Udalski, M. Zoccali, H. Bond, M. Albrow, I. Bond, T. Brown, M. Dominik, C. Fryer, M. Livio, S. Mao, and M. Rejkuba, Astrophys. J. **843**, 145 (2017).
[121] J. Ibanez, Astron. Astrophys. **124**, 175 (1983), https://ui.adsabs.harvard.edu/abs/1983A%26A...124..175I/abstract.
[122] I. Bray, Phys. Rev. D **34**, 367 (1986).
[123] S. A. Klioner, Sov. Astron. **35**, 523 (1991), https://ui.adsabs.harvard.edu/abs/1991SvA....35..523K/abstract.

[124] J. F. Glicenstein, Astron. Astrophys. **343**, 1025 (1999), https://ui.adsabs.harvard.edu/abs/1999A%26A...343.1025G/abstract.
[125] M. Sereno and F. De Luca, Phys. Rev. D **74**, 123009 (2006).
[126] M. C. Werner and A. O. Petters, Phys. Rev. D **76**, 064024 (2007).
[127] M. Sereno and F. De Luca, Phys. Rev. D **78**, 023008 (2008).
[128] A. B. Aazami, C. R. Keeton, and A. O. Petters, J. Math. Phys. (N.Y.) **52**, 092502 (2011).
[129] A. B. Aazami, C. R. Keeton, and A. O. Petters, J. Math. Phys. (N.Y.) **52**, 102501 (2011).
[130] G. He and W. Lin, Int. J. Mod. Phys. D **23**, 1450031 (2014).
[131] G. He, C. Jiang, and W. Lin, Int. J. Mod. Phys. D **23**, 1450079 (2014).
[132] X.-M. Deng, Int. J. Mod. Phys. D **24**, 1550056 (2015).
[133] G.-S. He and W.-B. Lin, Res. Astron. Astrophys. **15**, 646 (2015).
[134] X.-M. Deng, Int. J. Mod. Phys. D **25**, 1650082 (2016).
[135] G. He and W. Lin, Phys. Rev. D **93**, 023005 (2016).
[136] G. He and W. Lin, Phys. Rev. D **94**, 063011 (2016).
[137] G. He and W. Lin, Classical Quantum Gravity **34**, 105006 (2017).
[138] A. Bhadra and K. K. Nandi, Gen. Relativ. Gravit. **42**, 293 (2010).
[139] S. Ghosh and A. Bhadra, Eur. Phys. J. C **75**, 494 (2015).
[140] X.-M. Deng and Y. Xie, Phys. Lett. B **772**, 152 (2017).
[141] X.-M. Deng, Classical Quantum Gravity **35**, 175013 (2018).
[142] X.-M. Deng, Mod. Phys. Lett. A **33**, 1850110 (2018).
[143] G. Li and X.-M. Deng, Commun. Theor. Phys. **70**, 721 (2018).
[144] M. De Laurentis, R. De Rosa, F. Garufi, and L. Milano, Mon. Not. R. Astron. Soc. **424**, 2371 (2012).
[145] X.-M. Deng, Europhys. Lett. **120**, 60004 (2017).
[146] X.-M. Deng, Eur. Phys. J. Plus **132**, 85 (2017).
[147] I. De Martino, R. Lazkoz, and M. De Laurentis, Phys. Rev. D **97**, 104067 (2018).
[148] M. De Laurentis, I. De Martino, and R. Lazkoz, Phys. Rev. D **97**, 104068 (2018).
[149] M. De Laurentis, I. De Martino, and R. Lazkoz, Eur. Phys. J. C **78**, 916 (2018).
[150] J. Levin and G. Perez-Giz, Phys. Rev. D **77**, 103005 (2008).
[151] J. Levin and R. Grossman, Phys. Rev. D **79**, 043016 (2009).
[152] J. Levin and G. Perez-Giz, Phys. Rev. D **79**, 124013 (2009).
[153] J. Levin, Classical Quantum Gravity **26**, 235010 (2009).
[154] V. Misra and J. Levin, Phys. Rev. D **82**, 083001 (2010).
[155] B. Gao and X.-M. Deng, Ann. Phys. (Amsterdam) **418**, 168194 (2020).
[156] X.-M. Deng, Eur. Phys. J. C **80**, 489 (2020).
[157] X.-M. Deng, Phys. Dark Universe **30**, 100629 (2020).
[158] T.-Y. Zhou and Y. Xie, Eur. Phys. J. C **80**, 1070 (2020).